

# Fast X-ray flares from the quadruple system GT Muscae

L. Ducci<sup>1,2</sup>, S. Piraino<sup>1</sup>, H. M. Lübeck<sup>1</sup>, L. Ji<sup>1</sup>, A. Santangelo<sup>1</sup>, J. Schmitt<sup>3</sup>, C. Ferrigno<sup>2</sup>, E. Bozzo<sup>2</sup>

EBERHARD KARLS  
UNIVERSITÄT  
TÜBINGEN



<sup>1</sup>Institut für Astronomie und Astrophysik Tübingen (Germany)

<sup>2</sup>ISDC Data Center for Astrophysics, Versoix (Switzerland)

<sup>3</sup>Universität Hamburg, Hamburger Sternwarte (Germany)

ISDC  
DATA CENTRE FOR ASTROPHYSICS

hamburger  
sternwarte  
Fachbereich Physik I Universität Hamburg

## Abstract

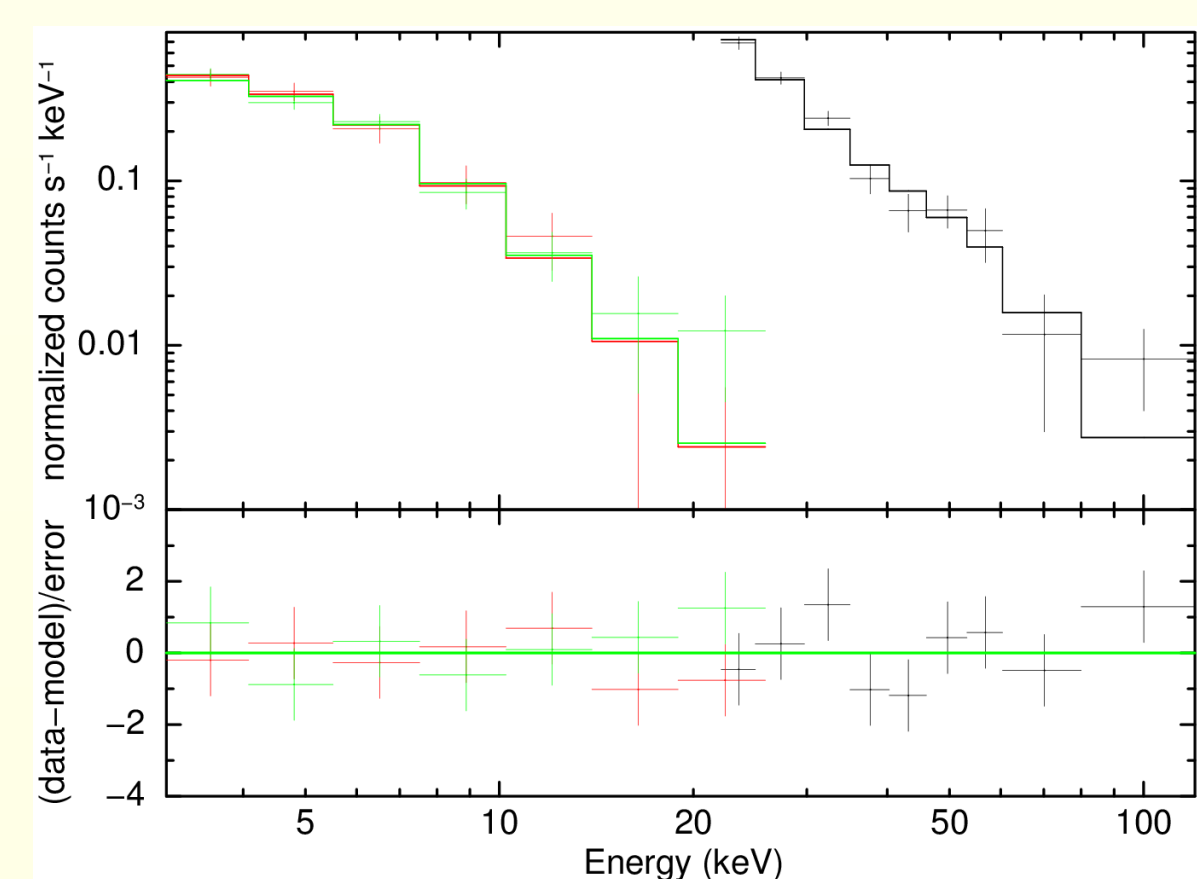
GT Muscae is a quadruple system hosting an RS CVn binary that shows a highly variable X-ray emission. We present a work based on the entire public archival INTEGRAL data set (exposure time: 11 Ms; energy range: 3-100 keV) which covers the period 2003-2017, and on the recent XMM-Newton observation of June 2016. The aims of this work are to study the temporal variability and spectral properties of GT Muscae and in particular its thermal component, and to detect and constrain the non-thermal hard X-ray emission component. In our preliminary work, we detected 11 bright flares which reached X-ray luminosities of  $10^{33}$  erg/s (3-100 keV). In three cases, we detected with the ISGRI instrument hard X-ray emission above 40 keV.

## RS CVn systems

RS CVn are detached binary systems composed of a chromospherically active F, G or K star, usually evolved, with a late-type main-sequence or subgiant companion (Audard et al. 2003). RS CVn rotate fast and have orbital periods of few days. These systems display a high level of activity with strong chromospheric line emissions and saturated coronal X-ray emissions ( $L_x/L_{bol} \sim 10^{-3}$ ). RS CVn display powerful energetic X-ray flares, with high temperatures (up to  $10^8$  K). The flares are likely produced by a sudden release of energy via magnetic reconnection (near the loop tops), which accelerates particles and causes subsequent plasma motions and heating. Thermal emission dominates X-ray emission, though in some large flares a nonthermal X-ray component might be observed. (Osten et al. 2016).

## INTEGRAL

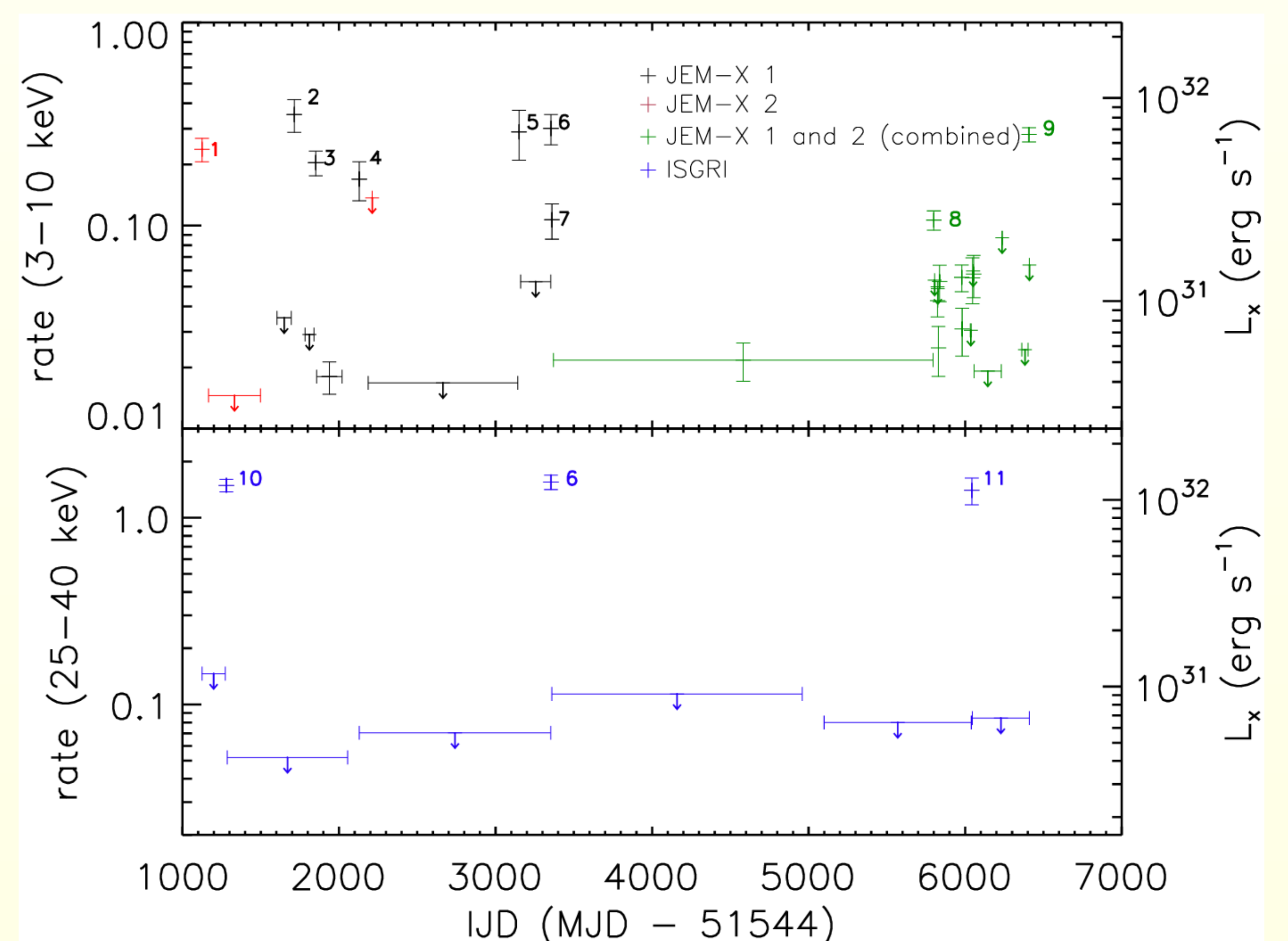
- **11 flares** (time scale: <1day) detected from 2003-2017;
- Flares #10, #11 only with ISGRI (outside FoV JEM-X);
- Quiescent luminosity:  $\sim 5 \times 10^{31}$  erg/s (3-50 keV; d=110pc from GAIA DR2)
- Average flare luminosity  $\sim 10^{33}$  erg/s (3-50 keV);
- Best fit of the average JEM-X+ISGRI spectrum during flares: 2 apec, absorbed.  $T_2 \sim 3 \times 10^8$  K consistent with highest  $T_2$  observed in other RS CVn binaries and flaring stars (e.g. Osten et al. 2016);
- **Alternatively, the hard X-ray tail detected by ISGRI can be attributed to nonthermal emission from a population of accelerated electrons.**



Parameters	
$N_H$ ( $10^{20}$ cm $^{-2}$ )	5.3 (fixed)
$kT_1$ (keV)	$5.0^{+1.1}_{-1.2}$
$EM_1$ ( $10^{55}$ cm $^{-3}$ )	$92^{+60}_{-20}$
$kT_2$ (keV)	$29^{+29}_{-12}$
$EM_2$ ( $10^{55}$ cm $^{-3}$ )	$3.6^{+5}_{-2}$
Abund	< 0.27
$\chi^2_{red}$ (d.o.f.)	0.813 (16)

Figure 1 (left): average JEM-X + ISGRI spectrum of GT Mus during flares and best-fitting parameters, with uncertainties at 68% c.i.

Figure 2 (right): JEM-X and ISGRI light curves of GT Mus, from 2003 to 2017. Error bars corresponds to 68% c.i. Downward arrows are  $3\sigma$  u.l.



## XMM-Newton

- **Best fit of the EPIC spectra: three VAPEC components absorbed by TBABS model;**
- Elemental abundances in Table 1 are relative to abundances from Asplund et al. (2009);
- GT Mus does not show significant X-ray variability during the observation;
- **X-ray luminosity (3-10 keV):  $5 \times 10^{31}$  erg/s: based on INTEGRAL results (Fig. 2), GT Mus was observed by XMM-Newton during a flare;**

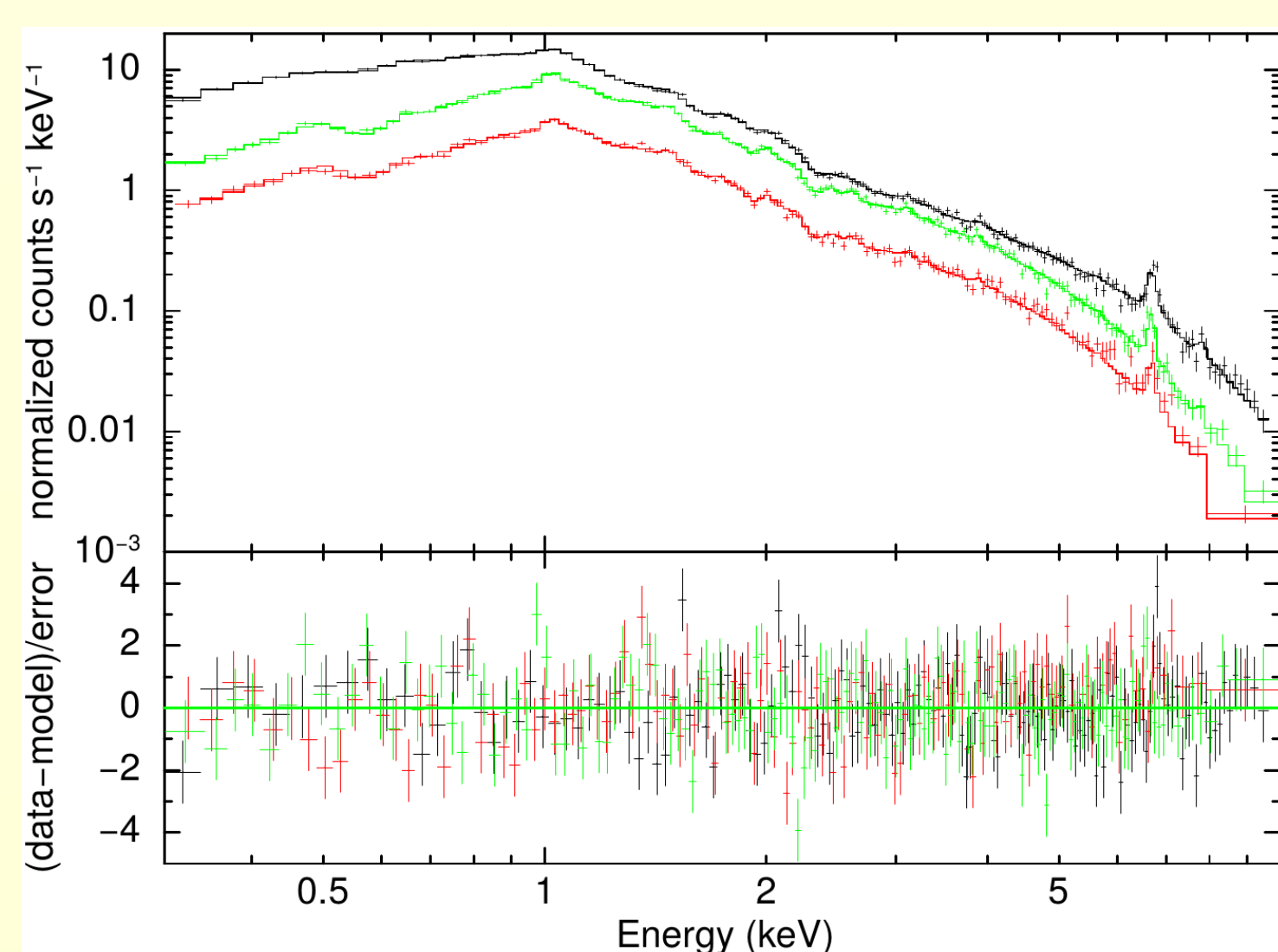


Figure 3: EPIC spectra (pn: black, MOS1: red, MOS2, green) of GT Mus, with residuals.

Table 1: Best-fitting parameters of the X-ray spectrum shown in Fig. 3. Errors at 68% c.i.

Parameters	
$N_H$ ( $10^{20}$ cm $^{-2}$ )	$5.3 \pm 0.3$
$kT_1$ (keV)	$0.79 \pm 0.02$
$EM_1$ ( $10^{54}$ cm $^{-3}$ )	$1.6 \pm 0.1$
$kT_2$ (keV)	$1.65 \pm 0.06$
$EM_2$ ( $10^{54}$ cm $^{-3}$ )	$5.7 \pm 0.7$
$kT_3$ (keV)	$4.7 \pm 0.3$
$EM_3$ ( $10^{54}$ cm $^{-3}$ )	$6.9 \pm 0.5$
C (abund.)	< 0.6
N	$1.05 \pm 1.03$
O	$0.57 \pm 0.08$
Ne	$1.26 \pm 0.17$
Mg	$0.36 \pm 0.05$
Al	$1.9 \pm 0.5$
Si	$0.35 \pm 0.04$
S	$0.29 \pm 0.06$
Ar	$0.8 \pm 0.2$
Ca	$0.71 \pm 0.19$
Fe	$0.25 \pm 0.02$
Ni	$0.8 \pm 0.2$
$\chi^2_{red}$ (d.o.f.)	1.1816 (420)
$L_x$ (0.5-10 keV)	$(1.535 \pm 0.006) \times 10^{32}$ erg s $^{-1}$
$L_x$ (3-10 keV)	$(4.930 \pm 0.007) \times 10^{31}$ erg s $^{-1}$

## Magnetic field strength and loop length

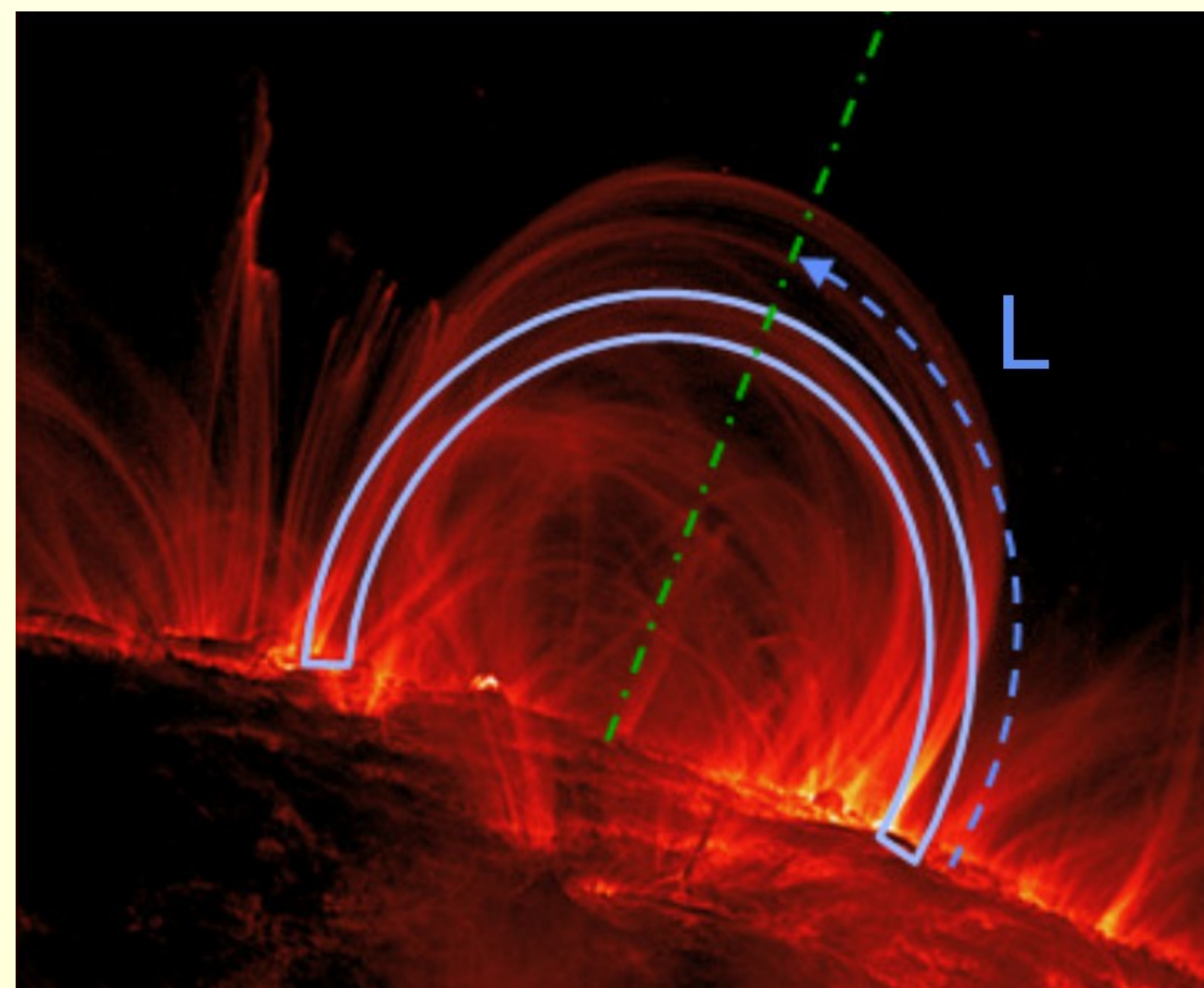


Figure 4: Loops from active regions on the surface of RS CVn extend into the stellar corona. The reconnection event occurring near the loop top is accompanied by a sudden release of energy, including X-ray emission. The plasma confined in a coronal loop can be described with a single coordinate ( $L$ ) along the loop (image adapted from Reale et al. 2010).

- The laws derived by Shibata & Yokoyama (2002) give expressions for the magnetic field strength  $B$  and characteristic length of the loop  $L$  in dependence of EM, temperature  $T$ , and pre-flare electron density  $n_0$ :

$$B(\text{PB}) = 50 \left( \frac{EM}{10^{48} \text{ cm}^{-3}} \right)^{-1/5} \left( \frac{n_0}{10^9 \text{ cm}^{-3}} \right)^{3/10} \left( \frac{T}{10^7 \text{ K}} \right)^{17/10} \text{ G},$$

$$L(\text{PB}) = 10^9 \left( \frac{EM}{10^{48} \text{ cm}^{-3}} \right)^{3/5} \left( \frac{n_0}{10^9 \text{ cm}^{-3}} \right)^{-2/5} \left( \frac{T}{10^7 \text{ K}} \right)^{-8/5} \text{ cm}.$$

- We use the best fit temperature and EM derived from single temperature model fitting the data (both XMM-Newton and INTEGRAL) to obtain a rough estimate of the loop length and magnetic field strength during the flares.

- Assuming  $n_0 = 10^9 \text{ cm}^{-3}$ , we obtain:  
XMM-Newton flare:  **$B \sim 51$  G;  $L \sim 3 \times 10^{11}$  cm;**  
INTEGRAL flares:  **$B \sim 97$  G;  $L \sim 1.4 \times 10^{12}$  cm;**

- $L$  is lower than or similar to the stellar radius of the component of the GT Mus system with largest radius, ( $33 R_{\text{sun}} = 2.3 \times 10^{12} \text{ cm}$ , Tsuboi et al. 2016).

## References

Asplund et al., 2009, ARAA 47, 481      Audard et al. 2003, A&A 398, 1137  
Osten et al. 2016, ApJ 832, 174      Tsuboi et al. 2016, PASJ 68, 90  
Shibata & Yokoyama 2002, ApJ 577, 422      Raassen et al. 2007, MNRAS 1075, 1082  
Reale et al. 2010, LRSP, 7, 5